Contribution from the Department of Chemistry and the Institute for Materials Research, McMaster University, Hamilton, Ontario, Canada L8S 4M1

New Mixed-Valence Europium Perovskites in the System Eu–Ta–O

J. E. GREEDAN,* H. F. GIBBS, and C. W. TURNER

Received August 24, 1976 AIC60611+

New mixed-valence europium tantalate perovskites have been prepared in the system Eu–Ta–O. The existence of a compound with composition close to $Eu^{II}_2(Eu^{III}Ta^{V})O_6$ is confirmed and some evidence for a limited solid solution, $Eu^{II}_2(Eu^{II}_xEu^{III}_{1-x}Ta)O_{3.0-x/2}$ where $0 < x \lesssim 0.10$, is presented. The nonexistence of $Eu^{II}_2(Eu^{II}Ta)O_{5.50}$ is also confirmed. A completely new series of phases described as $Eu^{II}(Eu^{II}_xEu^{III}_{0.50-3x/2}Ta^{V}_{0.50+x/2})O_{3.00}$ where $0 < x \lesssim 0.17$ has been prepared in a hydrogen atmosphere and in welded molybdenum crucibles under argon. $Eu_2(EuTa)O_6$ is possibly monoclinic, $P2_1/n$ [a = 5.803 (4) Å, b = 5.883 (4) Å, c = 8.238 (8) Å, β = 90.36°], but evidence has been found for a triclinic supercell probably $C\bar{1}$ [a = 11.653 (5) Å, b = 11.824 (6) Å, c = 8.2667 (7) Å, β = 90.19°, $\alpha \approx \gamma \approx 90°$]. This is contrary to previous reports. The phases $Eu^{II}(Eu^{II}_xEu^{III}_{0.50-3x/2}Ta^{V}_{0.50+x/2})O_{3.00}$ show an apparently continuous tendency toward simple cubic symmetry with increasing x with pseudocubic lattice constants decreasing from 4.144 to 4.125 Å. X-ray fluorescence, tga, and magnetic susceptibility measurements support the above formulation. Diffuse reflectance and low-temperature magnetization measurements give evidence for the simultaneous presence of Eu^{II} on both the A and B sites of these perovskites.

Introduction

In a recent study[1,2] three guidelines were identified which provide a semiquantitative means of predicting the stability of divalent europium in complex oxides: (i) Any proposed europium(II) oxide phase should have a Sr analogue. (ii) Other cations which would coexist with Eu^{II} must not be too easily reduced. (iii) Any proposed europium(II) oxide should not fall too near the boundary of the relevant structure stability field. In practice guidelines ii and iii are closely linked. Consider the nonexistence of Eu_3WO_6. Sr_3WO_6 exists as a distorted perovskite with Sr^{II} and W^{VI} on the 6-fold site and Sr^{II} on the 12-fold site. The requirement that the large Eu^{II} ion be present on the B site places the hypothetical Eu_3WO_6 in a relatively unstable position in the perovskite structure field. The phase assemblage actually found for the composition corresponding to Eu_3WO_6 is $Eu^{III}_6WO_{12}$, $Eu^{II}WO_4$, and W indicating some reduction of W^{VI} to W and oxidation of some Eu^{II} to Eu^{III}. It was in this context that we became interested in the Eu–Ta–O system.

Two strontium tantalate perovskites, $Sr_3TaO_{5.5}$[3] and Sr_2EuTaO_6,[4] had been reported suggesting the possible existence of the europium analogues $Eu^{II}_3TaO_{5.5}$ and $Eu^{II}_2Eu^{III}TaO_6$. Both strontium tantalates have Sr^{2+} on the 12-fold site in all cases and an ordered sharing of the 6-fold site between Sr^{II} and Ta^{V} for $Sr_2(SrTa)O_{5.5}$ and between Eu^{III} and Ta^{V} for $Sr_3(EuTa)O_6$. $Sr_2(SrTa)O_{5.5}$ is cubic, a_0 = 8.34 Å,[3] while $Sr_2(EuTa)O_6$ is reported to be monoclinic, a = 5.84 Å, b = 5.91 Å, c = 8.30 Å, β = 90° 12′.[4] The existence of $Eu_2(EuTa)O_{5.5}$ would require the presence of Eu^{II} on the 6-fold site, an interesting situation vis-à-vis guidelines ii and iii considering the possible existence of the competing phase $Eu^{II}_2Eu^{III}TaO_6$ with the smaller Eu^{III} ion on the B site.

In our earlier work[2] the compound $Eu^{II}_2(Eu^{III}Ta)O_6$ was reported but no structural information was given. Adachi et al.[5,6] have recently reported a cubic perovskite phase which they characterize as $Eu^{II}_2Eu^{III}TaO_6$ on the basis of x-ray, magnetic susceptibility, and tga data. They also reported the nonexistence of $Eu^{II}_3TaO_{5.5}$ and concluded that Eu^{II} cannot be stabilized on the 6-fold site. We confirm some of the results of Adachi et al. in this present work but extend the investigation of the Eu–Ta–O system near Eu_3TaO_6 to reveal quite complex behavior and the existence of new mixed-valence europium tantalates some of which appear to contain Eu^{II} on both the 12-fold and the 6-fold sites in a perovskite structure.

Experimental Section

Synthetic Procedures. Solid-state reactions were carried out using two distinct environments: a closed system using mixes of Eu_2O_3, Ta_2O_5, and Ta or EuO and Ta_2O_5 in welded Mo crucibles under purified argon and a flow system in which mixtures of Eu_2O_3 and Ta_2O_5 or Eu_3TaO_7 are reduced in a hydrogen stream. In both cases samples consisted of pellets pressed from prefired (1200 °C) metal oxide powders which were mechanically mixed using a Wig-L-Bug. Eu_2O_3 (99.9 and 99.99%) was obtained from Research Chemicals and Ta_2O_5 (99.9%) from Canadian Scientific Products. High-purity (99.95%) Mo tubing (Thermoelectron) and round stock (Bram Metallurgical) were used to fabricate crucibles which were arc-welded under purified argon. Crucibles and contents were fired using an rf induction furnace at temperatures from 1200 to 2200 °C.

In the hydrogen flow system the furnace temperature was automatically programmed to ensure reproducible heating and cooling conditions. Samples were "quenched" from the reaction temperature, usually 1375 °C, in the hydrogen stream by rapid cooling at rates of 1000 °C/h to 900 °C whence the cooling rate was controlled by the thermal inertia of the furnace.

Chemical Analysis. The samples were analyzed in the solid state by x-ray fluorescence (XRF) and tga methods. The Eu:Ta atomic ratio in each sample was determined by XRF using a ^{109}Cd γ-excitation source monitoring the $L\alpha_1$ fluorescence for Eu and $L\beta_1$ for Ta. A set of five standards comprised of pellets of reasonably homogeneous mechanical mixtures of Eu_2O_3 and Ta_2O_5 were prepared from Eu:Ta = 3.20–2.20. The pellets were counted twice, once on each side, and the intensities averaged to obtain a calibration curve. The estimated uncertainty in the Eu:Ta ratio is ±0.05. Samples were oxidized in air and the weight gain was recorded using a Stanton-Redcroft tga system.

X-Ray Diffraction. Powder data were obtained using a Philips diffractometer and a Debye–Scherrer camera with Cu Kα radiation using a Si standard, a_0 = 5.4301 Å. Single-crystal data were obtained using precession photography and the automated diffractometer, Syntex $P\bar{1}$ with Mo Kα radiation.

Magnetic Data. Susceptibility data were collected in the region from 4.2 to 300 K using a PAR vibrating-sample magnetometer. A small sphere of high-purity Ni was used as a standard.

Diffuse Reflectance. Diffuse-reflectance spectra were obtained using a Cary 14 spectrophotometer and an integrating sphere in the region from 750 to 350 nm. $MgCO_3$ and MgO were used as standards.

Results and Discussion

Attempts to Prepare Eu_3TaO_6 and $Eu_3TaO_{5.5}$ in a Welded Molybdenum Crucible. Eu_3TaO_6. The appropriate mixes were fired in welded molybdenum crucibles from 1200 to about 2200 °C for periods of up to 48 h at the lower temperatures and 5–12 h at the higher temperatures. Melting was observed above 2200 °C. The results from six runs using either $^3/_4Eu_2O_3 + {}^3/_{20}Ta_2O_5 + {}^1/_5Ta$ or $2EuO + EuTaO_4$, regardless of firing temperature, were the same. A two-phase product was found consisting of a *distorted* pervoskite phase as a major component and a fccub phase identified as Eu_3TaO_7. Phase indentification was done by x-ray diffraction. The relative amount of Eu_3TaO_7 could be reduced following high-temperature firings and intermediate regrinding and

refiring steps but not below an estimated 5%. This suggests that although the presence of Eu_3TaO_7 could be due in part to kinetic effects, especially in low-temperature preparations, there may be a more fundamental problem. That is, perhaps the stable perovskite phase under these conditions contains less Eu^{3+} and O^{2-} than expected for Eu_3TaO_6. This would require some Eu^{2+} on the B site in the form of a solid solution between Eu_3TaO_6 and $Eu_3TaO_{5.5}$ which would be represented as $Eu_2(Eu^{II}_xEu^{III}_{1-x}Ta)O_{6-x/2}$.

To test this hypothesis mixes corresponding to solid solutions with $x = 0.06$ and 0.10 were prepared and fired at 1800 °C for 5 h followed by melting at about 2200 °C. The phase with $x = 0.06$ still contained some Eu_3TaO_7 but the $x = 0.10$ phase could be prepared free of Eu_3TaO_7. The x-ray powder patterns of the perovskite phases in each preparation, $x = 0$, 0.06, and 0.10, were essentially identical. The x-ray data will be discussed more fully later on. Magnetic measurements provide some evidence for this hypothesis. The measured molar Curie constant, C_M, for the nominal $x = 0$ phase is 8.58. For $Eu_2(EuTa)O_6$ the theoretical C_M is 8.23, obtained as described previously.[7] A C_M of 8.60 corresponds to a solid-solution phase with $x = 0.10$. Note that the phase which Adachi et al. characterized as Eu_2EuTaO_6 also has a C_M of about 8.6.

The powder pattern for all perovskite phases prepared in welded crucibles near the composition Eu_3TaO_6 was perovskite-like but clearly showed distortions from cubic symmetry. It was identical in peak positions and similar in relative intensities with that for Sr_2EuTaO_6. A single crystal was selected from the melt of the nominal $x = 0$ phase and precession photographs were taken. A cell corresponding to that for Sr_2EuTaO_6 was found which appeared to be monoclinic, possible space group $P2_1/n$. Some weak reflections were also observed suggesting that the a and b axes should be doubled. Data were collected using a Syntex $P\bar{1}$ automated diffractometer with Zr-filtered Mo Kα radiation, and a least-squares fit of 15 high-angle reflections gave a cell with $a = 5.802 \pm 0.004$ Å, $b = 5.883 \pm 0.004$ Å, $c = 8.238 \pm 0.008$ Å, and $\beta = 90.36°$. Examination of systematic absences confirmed the space group as $P2_1/n$. The larger cell suggested in the photographs was also found with $a = 11.653 \pm 0.005$ Å, $b = 11.824 \pm 0.006$ Å, $c = 8.266 \pm 0.007$ Å, $\beta = 90.19°$, and $\alpha \approx \gamma \approx 90°$. Examination of systematic absences showed that the supercell was C centered ($h + k = 2n + 1$) and comparison of the intensities of hkl and $\bar{h}k\bar{l}$ pairs and of hkl and $\bar{h}\bar{k}\bar{l}$ pairs indicates the absence of a twofold axis but the presence of an inversion center leading to $C\bar{1}$. A full structure determination is currently under way and will be reported elsewhere.

It will be recalled that Adachi et al. reported a cubic $(NH_4)_3FeF_6$ structure, $a_0 = 8.309$ Å, for the phase which they characterize as $Eu_2(EuTa)O_6$. We find no evidence for a cubic phase near this composition when the preparations are carried out in welded Mo crucibles. The density of our $x \approx 0.10$ phase is 8.4 g/cm^3 and the oxidation weight gain is 2.1%, values very near those reported by Adachi.

$Eu_3TaO_{5.5}$. Mixes in the proportion $EuO:Ta_2O_5 = 6:1$ were fired at 1200 °C for 48 h and a portion of this material was melted at about 2100 °C. The x-ray powder patterns for both powder and melt showed a two-phase mixture consisting of a perovskite with positions and relative intensities very similar to those observed for our "Eu_3TaO_6" plus EuO. The presence of EuO was confirmed by magnetic susceptibility data which showed an anomaly near 70 K, the Curie point for EuO. Mössbauer spectra showed the presence of considerable Eu^{III}.[8] No free Ta metal could be detected in the x-ray powder pattern or by metallographic examination of the melted boule. This is somewhat surprising but the amount of Ta expected is rather small and could be missed by either detection method.

Table I. Eu:Ta Atomic Ratios and Pseudocubic Lattice Constants of Perovskite Phases as a Function of Reaction Time in Hydrogen at 1375 °C

Reaction time, h	Eu:Ta in perovskite product (±0.05)	a_0,[a] Å
8	2.98	4.144 (6)
16	2.75	4.137 (2)
28	2.48	4.128 (3)
48	2.35	4.125 (2)

[a] Observation of one very weak superlattice line suggests that these values should be doubled.

These observations confirm those of Adachi et al.,[5] who reported that $Eu_3TaO_{5.5}$ cannot be prepared. The composition of the distorted perovskite phase which may exist as solid solutions between Eu_3TaO_6 and $Eu_3TaO_{5.5}$ is not certain. As mentioned previously, magnetic evidence suggests the composition $Eu^{II}_{2.0}Eu^{II}_{0.10}Eu^{III}_{0.90}Ta_{1.00}O_{5.95}$ for one of the phases prepared here. It is not easy to verify this by chemical analysis or tga weight gain experiments. We have compared the x-ray powder pattern of the distorted perovskite phase with those of known compositions in the series $Sr_2(Sr_xEu_{1-x}Ta)O_{6-x/2}$. For the Sr analogues the distorted perovskite structure of Sr_2EuTaO_6 obtains out to $x = 0.15$ but the cubic structure is seen for $x = 0.20$ and beyond. All of this information indicates that the extent of solid solution is limited to about $x = 0.10$ or 0.15 at the most.

Preparations in a Hydrogen Flow System. These experiments were carried out to explore the stability of mixed-valence Eu–Ta–O phases in a highly reducing environment. Initial experiments involved preparation of Eu_3TaO_7 and subsequent reduction at various temperatures from about 1000 to 1400 °C. Later experiments were carried out using mechanical mixtures of prefired Eu_2O_3 and Ta_2O_5.

The lowest temperature for which a reaction was observed in these studies was about 920 °C. Under these conditions the reaction was particularly sluggish; a reaction time of 48 h produced only 20–30% conversion to a perovskite material. By trial and error it was determined that a reaction temperature greater than 1300 °C was required to obtain reasonable reaction rates: 1375 °C was found to be convenient and was used for most experiments. The reaction rate was dependent on the thermal history of the starting materials. A sample of Eu_3TaO_7 which has been subjected to repeated high-temperature firings was completely inert to reduction even at 1400 °C.

All preparations resulted in a two-phase product, a major perovskite phase which was brown or orange-brown and a bright yellow minor phase on the surface of the pellets or loose powder which was identified as $Eu_5Ta_4O_{15}$.[9] The yellow surface phase was easily removed by grinding and the underlying perovskite phase was examined by powder, XRD, XRF, tga, and magnetic susceptibility measurements.

In Table I the results of the XRF and XRD measurements are reported as a function of reaction time for a typical set of experiments. To ensure the homogeneity of the pellet it was common practice to interrupt the firing after 8 h, scrape the yellow film from the pellet, regrind, and refire. It is remarkable that the Eu:Ta atomic ratio of the perovskite phase decreases from 3.0 of the starting material (Eu_3TaO_4 or 3:1 Eu_2O_3–Ta_2O_5) as a function of reaction time.

The x-ray powder patterns of the products also show systematic changes with Eu:Ta ratio. These changes can be described most clearly with the aid of Figure 1 in which the three strongest lines of the powder pattern are shown as a function of Eu:Ta ratio. The indexing scheme is based on a primitive cubic or pseudocubic perovskite cell to facilitate comparisons. Only one very weak line, observed in the powder

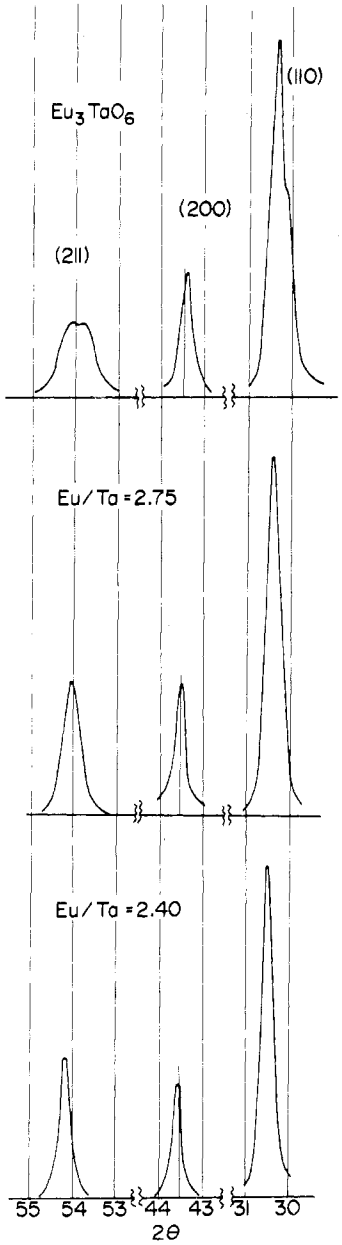

Figure 1. The three strongest lines in the powder pattern (Cu Kα) of the perovskite phases prepared in the hydrogen flow system as a function of Eu:Ta ratio.

patterns of some of these phases, suggested the existence of a superlattice requiring a doubling of the primitive cell. We also do not imply that any of the phases reported here are truly cubic. For convenience we shall refer to phases showing sharp low-angle ($2\theta < 60°$ (Cu K)) Bragg reflections as cubic, although even these phases show some broadening of high-angle reflections ($2\theta < 80°$). Phases which show broadening of low-angle lines will be classed as pseudocubic. Determination of the true symmetry of any of these materials will require very careful single-crystal x-ray or neutron powder work.

For compositions in the ratio range 3.0–2.9 the pattern is similar to that of Eu_3TaO_6 and is possibly monoclinic. From 2.8 to about 2.6 a pseudo cubic pattern is found in which the (110) splitting disappears and the (211) peak narrows but remains broad compared with (200). Below 2.5 an apparently cubic phase appears in which the (211) narrows. The pseudocubic lattice parameter of the perovskite phases decreases with decreasing Eu:Ta ratio as indicated in Table I.

Table II. Comparison of Analytical Data with the Solid-Solution Model: $Eu^{II}(Eu^{II}_xEu^{III}_{0.5-3x/2}Ta^{V}_{0.5-x/2})O_3$

Experiment			Theory		
Eu:Ta (±0.05)	C_M (±0.2)	% oxidn wt gain (±0.1%)	x	C_M	% oxidn wt gain (±0.1%)
2.98	8.10	2.0	0.0	8.23	2.2
2.68	8.54	2.1	0.05	8.57	2.3
2.42	9.40	2.3	0.17	9.38	2.5

Below Eu:Ta ≈ 2.4 lines from $Eu_5Ta_4O_{15}$ appear in the bulk phase as well as the surface layer. Compositions consistent with the observed Eu:Ta ratios assuming full oxygen stoichiometry can be represented as $Eu^{II}(Eu^{II}_xEu^{III}_{0.50-3/2x}Ta^{V}_{0.50+x/2})O_3$. Note that this requires a mixture of Eu^{II}, Eu^{III}, and Ta^{V} on the B site to satisfy charge neutrality. It is easily shown that Eu:Ta = $(3-x)/(1+x)$ indicating a decrease in Eu:Ta with increasing x. The trend toward cubic symmetry as well as the decrease in a_0 with decreasing Eu:Ta (increasing x) is then expected as the average radius of B-site ion decreases with decreasing Eu:Ta. Note that this compositional formula represents solid solution between $Eu^{II}(Eu^{III}_{0.50}Ta^{V}_{0.50})O_3$ and $Eu^{II}(Eu^{II}_{0.33}Ta^{V}_{0.67})O_3$ the latter of which does not exist independently under these conditions.

Support for the above formulation comes from additional syntheses carried out in welded Mo crucibles. Starting mixes consisting of Eu_2O_3, Ta_2O_5, and Ta were weighed out to correspond to $x = 0.10$, 0.15, 0.20, and 0.25 and were fixed at 1375 °C for 25 h. For $x = 0.10$ and 0.15 single-phase mixtures could be prepared after only one firing. The $x = 0.20$ composition contained a small amount of $Eu_5Ta_4O_{15}$ and the $x = 0.25$ phase a corresponding greater amount. Refiring of the latter two phases produced no changes and we conclude that the limit of solid solution is reached for $0.15 < x < 0.20$. The powder patterns and derived lattice constants of the $x = 0.10$ and 0.15 phases agree very well with similar compositions prepared in the hydrogen flow experiments.

For the sake of completeness we should note that another possible model is $Eu^{II}(Eu^{III}_{0.5-x}Ta^{IV}_{2x}Ta^{V}_{0.5-x})O_3$. This is also consistent with the observed decrease in a_0 and the degree of distortion from cubic symmetry with decreasing Eu:Ta. Unfortunately, the stability of Ta^{IV} in oxides is much less than that of Eu^{II}. Moreover, the magnetic data of Table II, in particular the increase in the Curie constant, C_M, with decreasing Eu:Ta, cannot be understood in terms of this model and it need not be considered further.

Representative compounds are listed in Table II along with observed and theoretical values for the magnetic Curie constant, C_M, and the weight gain on air oxidation. Reasonable agreement with the model $Eu^{II}(Eu^{II}_xEu^{III}_{0.50-3/2x}Ta^{V}_{0.50+x/2})O_3$ is observed except that the oxidation weight gain is somewhat low in all cases. This may be due to contamination by undetected phases such as Eu_3TaO_7 or $Eu_5Ta_4O_{15}$.

Evidence for Eu^{2+} on the B Site. As the analytical data, particularly the magnetic Curie constants, seem to demand the presence of Eu^{2+} on the B site as well as the A site, we have looked for corroborating evidence.

In Figure 2 are shown low-field magnetization vs. temperature data for various $Eu^{II}(Eu^{II}_xEu^{III}_{0.50-3x/2}Ta^{V}_{0.50+x/2})O_3$ phases below 4.2 K where these materials show magnetic ordering.

The lowest curve is that of $Eu^{II}(Lu_{0.5}Ta_{0.5})O_3$ a material with a cubic lattice constant comparable to those of the compounds of interest here ($a_0 = 4.100$ Å) and with Eu^{II} on the 12-fold site only. This compound is an antiferromagnet with $T_N = 4.0$ K.[10] The magnetization curve is normal for a polycrystalline antiferromagnet as $M(0) \approx {}^2/_3M(T_N)$. For increasing x the shape of the magnetization curve changes.

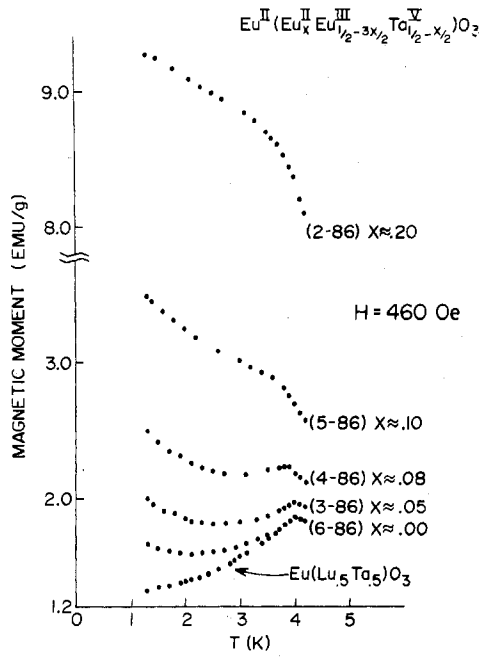

Figure 2. Low-temperature magnetization curves for various members of the system $Eu^{II}(Eu^{II}_{x}Eu^{III}_{0.50-3x/2}Ta^{V}_{0.50+x/2})O_{3.00}$ and $Eu(Lu_{0.5}Ta_{0.5})O_3$. Applied field is 410 Oe.

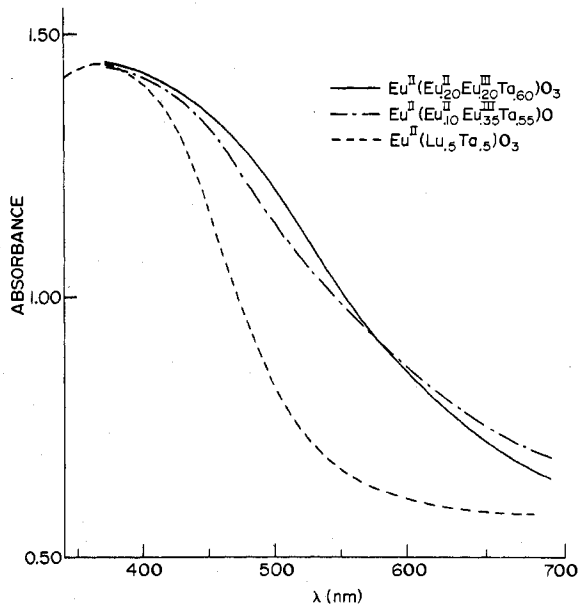

Figure 3. Diffuse reflectance spectra of $Eu^{II}(Eu^{II}_{0.10}Eu^{III}_{0.35}Ta^{V}_{0.55})O_3$ and $Eu^{II}(Eu^{II}_{0.20}Eu^{III}_{0.20}Ta_{0.60})O_3$ compared with that of $Eu(Lu_{0.5}Ta_{0.5})O_3$.

For low values of x a Néel point is still apparent at 4.0 K but a tail of increasing magnetization appears at low temperature and the value of the overall magnetic moment increases with increasing x. At $x \approx 0.08$ the Néel temperature appears to shift downward and is missing for $x \approx 0.10$ and 0.20. The magnetization curve for $x \approx 0.20$ is typical of a ferro- or ferrimagnetic material. More work is obviously required to understand the apparently complex magnetic properties of these phases. However, it is clear that systematic changes in magnetic structure occur with increasing x and that such changes can be understood only if Eu^{2+} is simultaneously present on both the A and the B sites. For example at low values of x most of the total Eu^{2+} resides on A sites giving rise to an antiferromagnetic structure, the expected result for an Eu^{2+} perovskite with such a lattice parameter.[10] The residual Eu^{2+} on the B site is coupled only weakly or not at all to A-site Eu^{2+} thus giving a paramagnetic "tail" at low temperatures. As the concentration of Eu^{2+} on the B site increases, coupling to the A-site ions becomes stronger, first causing a downward shift of the Néel point and finally its complete disappearance and the destruction of the A-site AF ordering by $x \approx 0.20$.

Diffuse-reflectance data are shown in Figure 3 for the near-UV–visible region. Again the lowest curve is that for $Eu^{II}(Lu_{0.5}Ta_{0.5})O_3$. The absorption reaches a maximum at about 370 nm and falls off quickly in the visible region. The other curves are for $Eu^{II}(Eu^{II}_{0.10}Eu^{III}_{0.35}Ta_{0.65})O_3$ and $Eu^{II}(Eu^{II}_{0.20}Eu^{III}_{0.20}Ta_{0.60})O_3$. For both of these one observes an absorption maximum at about 370–390 nm followed by additional strong absorption through the visible region with a possible shoulder at about 470–500 nm although the resolution is poor.

The absorption maximum at 370 nm observed for all compounds can be assigned with some confidence to the $4f^7 \rightarrow 4f^6 5d_{e_g}$ transition which is expected to be lowest lying for Eu^{2+} in the cubic (O_h) 12-fold site of perovskite. For Eu^{2+} in a cubic (O_h) 6-fold perovskite site the lowest lying transition should be $4f^7 \rightarrow 4f^6 5d_{t_{2g}}$. The relative position of these transitions in a real crystal will depend upon the relative magnitude of the crystal field splittings, Δ_A at the 12-fold and Δ_B at the 6-fold sites. The lowest lying transition will be associated with the site with the greatest Δ. If $\Delta_B > \Delta_A$, the additional absorption found in $Eu^{II}(Eu^{II}_{0.20}Eu^{III}_{0.20}Ta_{0.60})O_3$ and $Eu^{II}(Eu^{II}_{0.10}Eu^{III}_{0.50}Ta_{0.55})O_3$ could then be due to the $4f^7 \rightarrow 4f^6 5d_{t_{2g}}$ transition associated with Eu^{2+} on the B site.

Summary

We have prepared a number of new mixed-valence perovskite phases in the system Eu–Ta–O. These are of two types: those for which Eu:Ta = 3.00 and those for which 3.00 > Eu:Ta $\lesssim$ 2.40. A compound of stoichiometry close to $Eu^{II}_2(Eu^{III}Ta^{V})O_6$ was prepared and found to be monoclinic, $P2_1/n$, with the possibility of a triclinic, $C\bar{1}$, supercell. The lattice constants of the monoclinic cell agree well with those of the Sr analogue $Sr_2(Eu^{III}Ta^{V})O_6$. This finding is in conflict with that of Adachi et al., who reported a cubic Eu_3TaO_6, $Fm3m$. It is possible that Adachi's phase is a quenched high-temperature modification. We have also confirmed the report of Adachi that $Eu_3TaO_{5.5}$ does not exist under our synthetic conditions. Evidence from magnetic susceptibility measurements leads us to suspect that some limited solid solution exists between Eu_3TaO_6 and the nonexistent $Eu_3TaO_{5.5}$ and that the compound which is stable during preparations under Ar in welded Mo crucibles is close to $Eu^{II}_2(Eu^{II}_{0.10}Eu^{III}_{0.40}Ta_{0.50})O_{5.95}$. If syntheses are carried out under H_2 using Eu_3TaO_7 or mixtures of Eu_2O_3 and Ta_2O_5 as starting materials, perovskite products with Eu:Ta < 3.00 are obtained. These phases can be described as solid solutions between Eu_3TaO_6 [$Eu^{II}(Eu^{III}_{0.5}Ta^{V}_{0.5})O_3$] and a hypothetical phase $Eu_4Ta_2O_9$ [$Eu^{II}(Eu^{II}_{1/3}Ta^{V}_{2/3})O_3$]. This series of compounds shows a range of structures which vary with Eu:Ta ratio, monoclinically distorted perovskites being found for Eu:Ta $\approx$ 3.00 while true cubic symmetry is approached as Eu:Ta approaches 2.40. Below Eu:Ta = 2.40 a two-phase region appears involving $Eu_5Ta_4O_{15}$ plus perovskite. The magnetic and optical properties and XRF and tga data, as well as the aforementioned structural trends, are consistent with the solid-solution hypothesis.

The phases with Eu:Ta < 3.00 can also be prepared under Ar in welded Mo crucibles using the appropriate reaction mixtures of Eu_2O_3, Ta_2O_5, and Ta metal. The mechanism of Eu loss in the hydrogen flow experiments is not known but it may involve volatilization of Eu as in the well-known case of EuO which disproportionates at high temperatures under conditions of low pO_2 to Eu(v) + Eu_3O_4.[11]

Acknowledgment. We thank Professor K. Fritze for use of the XRF facility, Mr. R. Robertson for considerable advice and assistance with these measurements, Professor C. V. Stager for use of the magnetometer, Mr. J. Niemanis for the magnetic measurements, Mr. R. Faggiani for the precession photographs and the diffractometer data, and Professor C. Calvo for assistance in the interpretation of this data. We acknowledge several useful discussions with Professor Gregory J. McCarthy regarding possible phase relations in this complex system. The financial support of the Science and Engineering Research Board of McMaster University and the National Research Council of Canada is acknowledged.

Registry No. Eu_3TaO_7, 12444-76-7; Eu_3TaO_6, 55763-53-6; $Eu_3TaO_{5.5}$, 61075-76-1; $Eu(Lu_{0.5}Ta_{0.5})O_3$, 60923-91-3; $EuTaO_3$, 61075-74-9; $Eu_4Ta_2O_9$, 61075-75-0; Eu_2O_3, 1308-96-9; Ta_2O_5, 1314-61-0; Ta, 7440-25-7; EuO, 12020-60-9.

References and Notes

(1) G. J. McCarthy and J. E. Greedan, *Inorg. Chem.*, **14**, 772 (1975).
(2) J. E. Greedan, G. J. McCarthy, and C. Sipe, *Inorg. Chem.*, **14**, 775 (1975).
(3) L. H. Brixner, *J. Am. Chem. Soc.*, **80**, 3214 (1958).
(4) V. S. Filip'ev and E. G. Fesenko, *Sov. Phys.—Crystallogr.* (*Engl. Transl.*), **10**, 532 (1966).
(5) K. Sato, G. Adachi, and J. Shiokawa, *Mater. Res. Bull.*, **10**, 113 (1975).
(6) K. Sato, G. Adachi, and J. Shiokawa, *J. Inorg. Nucl. Chem.*, **38**, 1287 (1976).
(7) J. E. Greedan, R. G. Johnston, and G. J. McCarthy, *Inorg. Chem.*, **15**, 1238 (1976).
(8) C. L. Chien, private communication.
(9) J.-P. Fayalle and B. Raveau, *C. R. Hebd. Seances Acad. Sci., Ser. C*, **279**, 521 (1974).
(10) J. E. Greedan, R. G. Johnston, and C. L. Chien, *J. Solid State Chem.*, in press.
(11) J. M. Haschke and H. A. Eick, *J. Phys. Chem.*, **73**, 374 (1969).

Contribution No. 2415 from the Central Research and Development Department, Experimental Station, E. I. du Pont de Nemours and Company, Wilmington, Delaware 19898

Preparation and Properties of the Scheelite-Type $LnGe_{0.5}W_{0.5}O_4$ Compounds

L. H. BRIXNER

Received August 13, 1976 AIC60594O

The title compositions were prepared for all rare earth ions (except Pm) as well as for Ln being Y, La, and Bi. The Sc compound did not form and the Ga composition exhibits another structure. All materials studied (except Ga) crystallize in an undistorted, disordered scheelite structure, space group $I4_1/a$. The lattice parameters and excitation and emission spectra of the fluorescing compositions are reported.

Introduction

Compounds of the type $LnGe_{0.5}W_{0.5}O_4$ can be looked upon as IV–VI substitutions for pentavalent Nb^{5+} in the $LnNbO_4$ rare earth niobates. This type of substitution with Ti^{4+} in the unusual tetrahedral coordination was first described in 1964.[1] These $LnM_{0.5}Ti_{0.5}O_4$ compounds (where M can be either Mo^{6+} or W^{6+}) crystallize almost exclusively in the scheelite ($CaWO_4$) rather than in the fergosonite ($YNbO_4$) structure. Blasse[2] later also prepared some of these titanates as well as some of the equivalent germanates with Ln being La, Gd, Y, and Lu. $LnGe_{0.5}Mo_{0.5}O_4$ compounds with Ln being Pr, Nd, Gd, Tb, Dy, Ho, Er, and Yb were described by Finch et al.[3]

The present paper reports the preparation of all $LnGe_{0.5}W_{0.5}O_6$ rare earth compounds as well as the Ga, Y, La, and Bi compositions. The fluorescent behavior of the active ions Sm^{3+}, Eu^{3+}, Tb^{3+}, Dy^{3+}, and Tm^{3+} in $LaGe_{0.5}W_{0.5}O_4$ as a host is also described.

Experimental Section

All compounds were prepared by the standard solid-state technique of prefiring the stoichiometric constituent oxide components (GeO_2, electronic grade from Eagle Pitcher; WO_3, purified analytical grade from Fisher Scientific Co.; and Ln_2O_3, 99.99% from Research Co. Chemicals) at 1000 °C for 10–14 h, ball-milling and refiring at 1100 and 1200 °C for 4 h each. A single crystal of $LaGe_{0.5}W_{0.5}O_4$ was grown by the Czochralski technique from an Ir crucible in air. The melting point of this composition is 1526 °C, and excessive vaporization (GeO_2) occurred even at 150 psi. Since all other rare earth compounds would melt even higher, no attempts were made to grow those crystals.

The x-ray parameters were obtained by a least-squares treatment of d values read from Guinier-Hägg films. Fluorescence data were measured with a Perkin Elmer Model MPF-2A spectrophotometer.

Results and Discussion

A. Structure. Table I summarizes the lattice parameters, cell volumes, and calculated x-ray densities of the studied compounds. The cell edges marked with asterisks are those previously reported by Blasse[2] and are in good agreement. As one can see, all of the rare earth compounds, including Y and La, do crystallize in the same structure. This is in contrast to the three different structural types occurring, for instance, in the $Ln_2(MoO_4)_3$ molybdates.[4] Other rare earth series, such as the niobates,[5] also exhibit only one structural prototype. As mentioned earlier, the Ga composition crystallizes in different, orthorhombic symmetry, space group *Pbcn* (D_{2h}^{14}), point group *mmm*. Since according to Shannon[6] Ga^{3+} in octahedral coordination has a radius of 0.62 Å and the smallest rare earth (Lu) has one of 0.86 Å, the size limitation for the stability of the scheelite structure for the $LnGe_{0.5}W_{0.5}O_4$ type must be somewhere between these two numbers. The fact that $LuGe_{0.5}W_{0.5}O_4$ still does form a scheelite is surprising, since in the case of the pure tungstates Cd^{2+} (0.95 Å) in $CdWO_4$ already crystallizes in the different wolframite ($P2/a$) structure.

If one plots the cube of Shannon's[6] radii vs. the cell volume, an excellent straight-line relationship is obtained as seen in

Table I. Lattice Parameters and Densities of the $LnW_{0.5}Ge_{0.5}O_4$ Compounds[a]

Compn	a_0, Å	c_0, Å	ρ, g ml^{-1}
$YW_{0.5}Ge_{0.5}O_4$	5.089	11.089	6.50_2
$LaW_{0.5}Ge_{0.5}O_4$	5.266	11.813	6.71_3
$CeW_{0.5}Ge_{0.5}O_4$	5.220	11.620	6.97_1
$PrW_{0.5}Ge_{0.5}O_4$	5.219	11.572	7.01_7
$NdW_{0.5}Ge_{0.5}O_4$	5.203	11.486	7.25_5
$SmW_{0.5}Ge_{0.5}O_4$	5.170	11.356	7.49_5
$EuW_{0.5}Ge_{0.5}O_4$	5.152	11.307	7.61_8
$GdW_{0.5}Ge_{0.5}O_4$	5.141	11.257	7.80_6
$TbW_{0.5}Ge_{0.5}O_4$	5.122	11.195	7.94_1
$DyW_{0.5}Ge_{0.5}O_4$	5.107	11.149	8.10_2
$HoW_{0.5}Ge_{0.5}O_4$	5.094	11.098	8.23_6
$ErW_{0.5}Ge_{0.5}O_4$	5.079	11.098	8.39_0
$TmW_{0.5}Ge_{0.5}O_4$	5.061	10.998	8.51_4
$YbW_{0.5}Ge_{0.5}O_4$	5.045	10.956	8.69_7
$LuW_{0.5}Ge_{0.5}O_4$	5.035	10.926	8.80_5
$BiW_{0.5}Ge_{0.5}O_4$	5.215	11.596	8.44_7

[a] $GaW_{0.5}Ge_{0.5}O_4$ crystallized in orthorhombic symmetry with $a = 9.503$ Å, $b = 9.634$ Å, and $c = 13.352$ Å.